J Membrane Biol (2015) 248:103–115
DOI 10.1007/s00232-014-9747-8

Effects of Ibandronate Sodium, a Nitrogen-Containing Bisphosphonate, on Intermediate-Conductance Calcium-Activated Potassium Channels in Osteoclast Precursor Cells (RAW 264.7)

Sheng-Nan Wu · Yan-Ming Huang · Yu-Kai Liao

Received: 27 July 2014 / Accepted: 23 October 2014 / Published online: 2 November 2014

Abstract Ibanonate sodium (Iban), a nitrogen-containing bisphosphonate, is recognized to reduce skeletal complications through an inhibition of osteoclast-mediated bone resorption. However, how this drug interacts with ion channels in osteoclasts and creates anti-osteoclastic activity remains largely unclear. In this study, we investigated the possible effects of Iban and other related compounds on ionic currents in the osteoclast precursor RAW 264.7 cells. Iban suppressed the amplitude of whole-cell K^+ currents (I_K) in a concentration-dependent manner with an IC_{50} value of 28.9 μM. The I_K amplitude was sensitive to block by TRAM-34 and Iban-mediated inhibition of I_K was reversed by further addition of DCEBIO, an activator of intermediate-conductance Ca^{2+}-activated K^+ (IK_{Ca}) channels. Intracellular dialysis with Iban diminished I_K amplitude and further addition of ionomycin reversed its inhibition. In 17β-estradiol-treated cells, Iban-mediated inhibition of I_K remained effective. In cell-attached current recordings, Iban applied to bath did not modify single-channel conductance of IK_{Ca} channels; however, it did reduce channel activity. Iban-induced inhibition of IK_{Ca} channels was voltage-dependent. As IK_{Ca}-channel activity was suppressed by KN-93, subsequent addition of Iban did not further decrease the channel open probability. Iban could not exert any effect on inwardly rectifying K^+ current in RAW 264.7 cells. Under current-clamp recordings, Iban depolarized the membrane of RAW 264.7 cells and DCEBIO reversed Iban-induced depolarization. Iban also suppressed lipopolysaccharide-stimulated migration of RAW 264.7 cells in a concentration-dependent manner. Therefore, the inhibition by Iban of IK_{Ca} channels would be an important mechanism underlying its actions on the functional activity of osteoclasts occurring in vivo.

Keywords Osteoclast · Ibandronate · Bisphosphonate · K^+ current · Intermediate-conductance Ca^{2+}-activated K^+ channel · Membrane potential · Cell migration

Introduction

Biphosphonates are stable analogs of pyrophosphates with a complex effect on the bone metabolism. Ibandronate (Iban), a commonly used bisphosphonate, has been approved for the treatment of postmenopausal osteoporosis characterized by a high rate of bone resorption and is associated with significant and sustained reduction in risk of vertebral and non-vertebral fractures (Fisher et al. 2013; Gallagher and Tella 2013; Mosekilde et al. 2013). It has been previously reported that Iban-mediated osteonecrosis could be connected with the activity of osteoclasts or macrophages (Pazianas 2010). Several reports have demonstrated that this drug can target osteoclasts in the bone microenvironment, thereby inhibiting cellular ability to resorb bone (Fisher et al. 2013; Marathe et al. 2011; Zhang et al. 2013). The inhibitory effect on osteoclasts arises from a mechanism through their inhibition of the farnesyl pyrophosphate synthase, which may lead to an increased

Electronic supplementary material The online version of this article (doi:10.1007/s00232-014-9747-8) contains supplementary material, which is available to authorized users.

S.-N. Wu (✉) · Y.-M. Huang · Y.-K. Liao
Department of Physiology, National Cheng Kung University Medical College, No. 1 University Road, Tainan City 70101, Taiwan
e-mail: snwu@mail.ncku.edu.tw

S.-N. Wu
Institute of Basic Medical Sciences, National Cheng Kung University Medical College, Tainan City, Taiwan

bone density (Ebetino et al. 2011; Fisher et al. 2013; Pazianas 2010; Prokopenko et al. 2014). Alternatively, the activity of membrane ion channels has been notably proposed to be the essential targets for different anti-resorptive drugs including bisphosphonates, (Jones and Birchard 2014; Komarova et al. 2001; Shao et al. 2005; Valverde et al. 2005). However, the ionic mechanisms of Iban action in osteoclasts are still incompletely understood.

The intermediate-conductance Ca^{2+}-activated K^+ (IK_{Ca}) channels (also known as $K_{Ca}3.1$, SK4, IKCa1, or KCNN4) are encoded by the KCNN4 gene. They have been studied in many non-excitable or neoplastic cells with the regard to their mechanisms linked to hormonal secretion, cell motility, cell proliferation, and regulation of Ca^{2+} influx and/or K^+ efflux (Begenisich et al. 2004; Diaz et al. 2014; Jensen et al. 2001; Liu et al. 1998; Jones and Birchard 2014; Kaushal et al. 2007; Lallet-Daher et al. 2009; McFerrin et al. 2012; Ohya et al. 2011; Shen et al. 2007; Valverde et al. 2005; Wulff et al. 2007). These channels have single-channel conductance of 20–60 pS and their pharmacological profile of IK_{Ca} channels is quite distinguishable from those of large- or small-conductance Ca^{2+}-activated K^+ channels (Begenisich et al. 2004; Espinosa et al. 2002; Jensen et al. 2001; Shen et al. 2007; Wulff et al. 2007). The modulators of IK_{Ca} channels represent a potentially therapeutic approach to a variety of pathological states including osteoporosis (Grössinger et al. 2014; Komarova et al. 2001; Ohya et al. 2011; Toyama et al. 2008; Valverde et al. 2005).

The RAW 264.7 cells, which belong to an Abelson leukemia virus transformed cell line, have been known to act as osteoclast progenitors as they can differentiate into osteoclasts in response to either lipopolysaccharide (LPS) or receptor activation of nuclear factor κB ligand (Islam et al. 2007; Wang et al. 2012). They are recognized as a suitable model for investigations of the functional activities in osteoclasts. Earlier reports have described the electrical properties of these cells (Espinosa et al. 2002; Jones and Birchard 2014; Komarova et al. 2001; Tsai et al. 2013). However, whether Iban and other related compounds can interact with ion channels to perturb ionic currents, membrane potential and cell behavior of these cells are still not fully studied.

Therefore, in this study, we sought to investigate whether Iban exerts any effects on ion channels, particularly on IK_{Ca} channels, in RAW 264.7 osteoclast progenitor cells and to address the issue of how this drug influences any effects on membrane potential and cell migration. It is possible from our results that the perturbation by Iban of IK_{Ca} channels are important mechanisms through the ability of this drug and its structurally related compounds to interfere with the resorptive activity of osteoclasts, if similar findings occur in vivo. The data also raise the possibility of its effects on other types of cells that clearly express $K_{Ca}3.1$ channels (Begenisich et al. 2004; Diaz et al. 2014; Kaushal et al. 2007; Lallet-Daher et al. 2009; McFerrin et al. 2012; Ohya et al. 2011; Toyama et al. 2008).

Materials and Methods

Drugs and Solutions

Ibandronate sodium (Iban; $C_9H_{22}NO_7P_2Na{\cdot}H_2O$; Bonviva®) was obtained from Hoffmann-La Roche Ltd. (Basel, Switzerland). Clotrimazole, DCEBIO (5,6-dichloro-1-ethyl-1, 3-dihydro-2*H*-benzimidazol-2-one), KN-93 (*N*-[2-[[[3-(4-chlorophenyl)-2-propenyl]methylamino]methyl]phenyl]-*N*-(2-hydroxyethyl)-4-methoxybenzenesulphonamide), and TRAM-34 (1-((2-chlorophenyl) (diphenyl)methyl)-1*H*-pyrazole) were purchased from Tocris Cookson Ltd. (Bristol, UK), and apamin, 17β-estradiol, iberiotoxin, ionomycin, and lipopolysaccharide (LPS) were from Sigma-Aldrich Inc. (St. Louis, MO). Chlorotoxin and margatoxin were kindly provided by Dr. Woei-Jer Chuang (Department of Biochemistry, National Cheng Kung University Medical College, Tainan City, Taiwan). All culture media, fetal bovine serum (FBS), L-glutamine, trypsin, and penicillin–streptomycin were obtained from Invitrogen (Carlsbad, CA). All other chemicals including $MgCl_2$ and $BaCl_2$ were commercially available and of reagent grade. Deionized water used in all experiments was made from a Milli-Q water purification system (Millipore, Bedford, MA).

The composition of bathing solution (i.e., normal Tyrode's solution) was 136.5 mM NaCl, 5.4 mM KCl, 1.8 mM $CaCl_2$, 0.53 mM $MgCl_2$, 5.5 mM glucose, and 5.5 mM HEPES–NaOH buffer, pH 7.4. To measure K^+ currents or membrane potential, the patch pipette was filled with a solution consisting of 130 mM K-aspartate, 20 mM KCl, 1 mM KH_2PO_4, 1 mM $MgCl_2$, 3 mM Na_2ATP, 0.1 mM Na_2GTP, 0.1 mM EGTA, and 5 mM HEPES–KOH buffer, pH 7.2. To avoid the contamination of Cl^- currents, Cl^- ions inside the pipette solution were replaced with aspartate. For the recordings of intermediate-conductance Ca^{2+}-activated K^+ (IK_{Ca}) channels, the pipette solution contained 145 mM KCl, 2 mM $MgCl_2$, and 5 mM HEPES–KOH, pH 7.2. In another set of whole-cell recordings, the recording pipette was filled with a solution containing 10 μM Iban. The pipette solution was commonly filtered on the day of use with a 0.22 μM pore size syringe filter (Millipore).

Cell Preparations

RAW 264.7 cell line, an osteoclast progenitor, was obtained from the American Type Culture Collection (TIB-71; Manassas, VA). They were routinely grown in phenol red-free Dulbecco's modified Eagle's medium (DMEM) supplemented with 10 % heat-inactivated FBS, 100 U/ml penicillin, and 10 μg/ml streptomycin. Cells were maintained in a 95 % air and 5 % CO_2 humidified atmosphere at 37 °C (Tsai et al. 2013; Wang et al. 2012). For subculturing, cells were trypsin-dissociated and passaged every 2–3 days. In some set of experiments, cells were treated with 1 μM 17β-estradiol for 12 h. Cell viability was evaluated using a WST-1 assay and an ELISA reader (Dynatech, Chantilly, VA).

RNA Isolation and Reverse Transcriptase-Polymerase Chain Reaction (RT-PCR)

To detect the expression of KCNN4 ($K_{Ca}3.1$) channel mRNA in RAW 264.7 cells, a semi-quantitative RT-PCR assay was performed. Total RNA samples were extracted from cells according to TRIzol reagent protocol (Invitrogen) and reverse transcribed into complementary DNA using Superscript II reverse transcriptase (Invitrogen). The sequences of forward and reverse primers for KCNN4 were as follows: KCNN4-f, 5′-ACC TTT CAG ACA CAC TTT GG-3′; and KCNN4-r, 5′-TCT CTG CCT TGT TAA ACT CC-3′. The PCR cycling conditions were 35 cycles of 95 °C for 2 min, 95 °C for 20 s, 60 °C for 20 s, and 72 °C for 10 min. The PCR products were made on 1.5 % (w/v) agarose gel containing ethidium bromide and then visualized under ultraviolet trans-illumination. Optical densities of DNA bands were scanned and quantified by AlphaImager 2200 (ProteinSimple; Santa Clara, CA).

Migration Assay

Chemotactic migration ability of RAW 264.7 cells was analyzed by a 64-well Boyden chamber (AP48; Neuro Prob Inc., Gaithersburg, MD). Cells were cultured in serum-free medium for 12 h. Thereafter, 1×10^7 cells/well were suspended in serum-free DMEM with indicated drugs and placed into the upper chamber of Boyden chamber with a polycarbonate filter (8 μM pore size; GE osmonics labstore, MN). The lower chamber was filled with a medium containing 10 % FBS (as a chemoattractant) and indicated drugs. The indicated drugs loaded into both the upper and lower chambers are LPS, EGTA or Iban. After being incubated for indicated times, cells in the upper chamber were cleaned off with a cotton swab. The cells present on the lower surface of the filters were fixed with methanol for 10 min. Filters were stained with hematoxylin (Vector Laboratories, CA) for 30 min. Subsequently, the nuclei stained in brown color cells in three different fields of each well were imaged at 20×, counted and averaged as a representative number of migrated cells per field.

Electrophysiological Measurements

Shortly before the experiments, the RAW 264.7 cells at confluence were dissociated with 0.25 % trypsin in 0.02 % EDTA, and a small aliquot of cell suspension was transferred to a recording chamber mounted on the stage of an inverted CKX-41 microscope (Olympus, Tokyo, Japan). The microscope was coupled to a video camera system with magnification up to 1,500× in order to monitor cell size during the experiments. Cells were immersed at room temperature (20–25 °C) in normal Tyrode's solution which contained 1.8 mM $CaCl_2$. The patch pipettes were made of Kimax-51 capillary tubes (Kimble, Vineland, NJ) using a PP-830 puller (Narishige, Tokyo, Japan) or a P-97 Flaming/Brown electrode puller (Sutter, Novato, CA). Their tips were fire-polished with an MF-83 microforge (Narishige), and the resistances ranged between 3 and 5 MΩ when pipettes were filled with different intracellular solutions described above. The signals recorded in cell-attached, inside-out, or whole-cell mode were measured by standard patch-clamp technique by means of an RK-400 (Bio-Logic, Claix, France) or an Axopatch 1D patch-clamp amplifier (Molecular Devices, Sunnyvale, CA) (Shen et al. 2007; Wu et al. 2011). The offset potential between the pipette and bath solution was compensated with amplifier after the pipette entered the bath but immediately before a seal was made. Tested agents were applied by perfusion or added to the bath to obtain the final concentrations indicated.

Data Recordings and Analyses

The data were stored in a TravelMate-6253 laptop computer (Acer, Taipei, Taiwan) at 10 kHz through Digidata-1440A interface (Molecular Devices) which was controlled by pCLAMP 10.2 software (Molecular Devices). Current signals were low-pass filtered at 3 kHz. The voltage-step profiles with rectangular or ramp pulses created from pCLAMP 10.2 were employed to determine the current–voltage (*I–V*) relations for ion currents in RAW 264.7 cells. Some signals digitally stored through a wired USB or a wireless Bluetooth (He et al. 2013) were subsequently analyzed using different tools including pCLAMP 10.2, LabChart 7.0 program (AD Instruments; Gerin, Tainan, Taiwan) (Shin et al. 2011), Origin 8.0 (OriginLab, Northampton, MA), and custom-made macro-procedure embedded in Excel 2013 under Windows 7 (Microsoft, Redmond, WA).

To calculate concentration-dependent inhibition of Iban on the amplitude of I_K, each cell was held at −50 mV and the depolarizing pulses to +50 mV were applied. Current amplitudes at the level of +50 mV were measured during cell exposure to different concentrations (3 μM–1 mM), and they were compared with those measured after subsequent addition of TRAM-34 (3 μM). TRAM-34 is known to be a selective blocker of IK_{Ca} channels (Jensen et al. 2001; Wulff et al. 2000). The concentration required to suppress 50 % of I_K amplitude was then determined by means of a Hill function:

$$\text{Percentage inhibition} = \frac{E_{max} \times [C]^{n_H}}{IC_{50}^{n_H} + [C]^{n_H}},$$

where $[C]$ is the Iban concentration, IC_{50} and n_H are the concentration required for a 50 % inhibition and the Hill coefficient, respectively, and E_{max} is the maximal decrease in current amplitude (i.e., TRAM-34-sensitive current) caused by Iban.

With the aid of Chem3D and ChemDraw programs embedded in ChemBiol3D Ultra version 14 (PerkinElmer; Waltham, MA), the different parameters for Iban/Na and Iban/Ca complexes involved in regulation of IK_{Ca} channels, such as torsion energy, 1,-4-Van der Waals force, and bend, stretch and stretch-bend energies, were calculated (So et al. 2011).

Single-Channel Analyses

The amplitudes of single IK_{Ca}-channel currents were analyzed using pCLAMP 10.2. Multi-gaussian adjustments of the amplitude distributions among channels were created to determine unitary currents (Kemmer and Keller 2010). The functional independence among channels was commonly validated by comparing the observed stationary probabilities with the values calculated according to binominal law. The number of active channels in the patch was evaluated at the end of each experiments and then used to normalize the channel open probability at each potential. The probabilities of IK_{Ca}-channel openings were estimated using an iterative process to minimize the χ^2 calculated with a sufficiently large number of independent observations. The single-channel conductance of IK_{Ca} channels with or without addition of Iban was estimated by a linear regression using mean unitary amplitudes measured at different levels of voltage.

To evaluate the voltage dependence of the inhibitory effect of Iban on the activity of IK_{Ca} channels, the ramp pulses from −120 to +100 mV with a duration of 2 s were repetitively applied. The activation curve was calculated by averaging current traces evoked in response to 20 ramp pulses and subsequently by dividing each point of the mean current by single-channel amplitude for given voltage after the leakage currents were corrected. In the absence and presence of Iban, the probability of IK_{Ca}-channel openings measured at different membrane potentials was evaluated and then fit by the Woodhull equation (Clark et al. 1995; Dunn 1998). That is,

$$\frac{NP}{NP_0} = 1 + \frac{B}{K_0 \exp\left(\frac{F\delta V}{RT}\right)},$$

where NP_0 is the channel open probability in the absence of Iban at given membrane potential, K_0 is the equilibrium constant at 0 mV, B is the blocker (i.e., Iban) concentration, V is the membrane potential in mV, F is Faraday's constant, R is the universal gas constant, T is the absolute temperature, and δ is the fraction of the membrane voltage sensed at the binding site (i.e., the effective valence for a monovalent blocker).

Statistical Analyses

The averaged results are presented as the mean values ± standard error of the mean (SEM) with sample sizes (n) indicating the cell number from which the data were taken, and the error bars shown in each figure are plotted as SEM. The paired or unpaired Student's t tests were used for the statistical analyses. Assuming that the statistical difference among different groups was necessarily evaluated, analyses of variance with Duncan's multiple-range test for multiple comparisons were further implemented. The confidence assessment of best-fit parameter values (e.g., IC_{50}) was made (Kemmer and Keller 2010). Statistical analyses were generally performed using SPSS 17.0 (SPSS Inc., Chicago, IL). Statistical significance was determined at a P value of <0.05.

Results

The mRNA Expression for KCNN4 ($K_{Ca}3.1$) in RAW 264.7 Cells

As the IK_{Ca} channels are products of KCNN4 gene, we first examined the expression level of KCNN4 mRNAs on RAW 264.7 cells. The mRNA expression of KCNN4 was performed by use of a semi-quantitative RT-PCR assay. As shown in Fig. 1, our RT-PCR analysis presented the mRNA of KCNN4 in RAW 264.7 cells. Therefore, under our experimental conditions, the expression of KCNN4-encoded channels inherently in these cells can be detected and is not lost in culture.

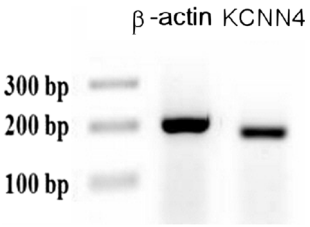

Fig. 1 The expression of KCNN4 ($K_{Ca}3.1$) mRNAs isolated from RAW 264.7 cells. Total RNA was isolated and RT-PCR analysis was carried out. Amplified RT-PCR products were obtained for a marker lane of DNA molecular size (*leftmost lane*), and for β-actin and KCNN4 in RAW 264.7 cells. The target sequence for KCNN4 was described under "Materials and Methods" section. Note that mRNA expression of KCNN4 was clearly detected in RAW 264.7 cells

Inhibitory Effect of Iban on Voltage-Gated K^+ Current (I_K) Measured from RAW 264.7 Cells

In the initial set of electrophysiological experiments, we evaluated the effect of Iban on I_K in these cells under the whole-cell configuration described under Materials and Methods. As RAW 264.7 cells were immersed in normal Tyrode's solution containing 1.8 mM $CaCl_2$, the I_K in response to a 1-sec ramp pulse from −100 to +50 mV could be readily elicited. After the cells were exposed to Iban, the amplitude of I_K evoked by the 1-sec long ramp pulse became progressively decreased (Fig. 2). For example, at the level of +50 mV, ARE at a concentration of 10 μM reduced I_K amplitude by 50 ± 4 % from 205 ± 26 to 102 ± 19 pA ($n = 9$, $P < 0.05$). After washout of ARE, current amplitude at the same level returned to 185 ± 28 pA ($n = 7$). However, neither chlorotoxin (1 μM) nor margatoxin (1 μM) could significantly suppress I_K in these cells. Chlorotoxin, a scorpion toxin, is reported to block Cl^- channels and margatoxin can suppress $K_V1.3$-encoded current.

The relationship between the Iban concentration and the percentage inhibition of I_K was derived and thereafter constructed. In these experiments, each cell was held at −50 mV, the ramp pulses from −100 to +50 mV with a duration of 1 s were applied, and current amplitudes at +50 mV in the absence and presence of different concentrations of Iban were measured. As illustrated in Fig. 2b, Iban (3 μM–1 mM) suppressed I_K amplitude in a concentration-dependent manner. With the use of a nonlinear least-squares fit to the data, the IC_{50} value required for the inhibitory effect of Iban on I_K in RAW 264.7 cells was calculated to be 28.9 μM, and this drug at a concentration of 1 mM nearly abolished current amplitude. In the SSR plot shown in inset of Fig. 2b, a horizontal line at SSR = 9.3 $\%^2$ was also made to determine the two IC_{50} values (Kemmer and Keller 2010). For a 95 % confidence interval, the lower and upper values amounted to 27.01 and 30.98 μM, respectively. Because of a steep slope on both

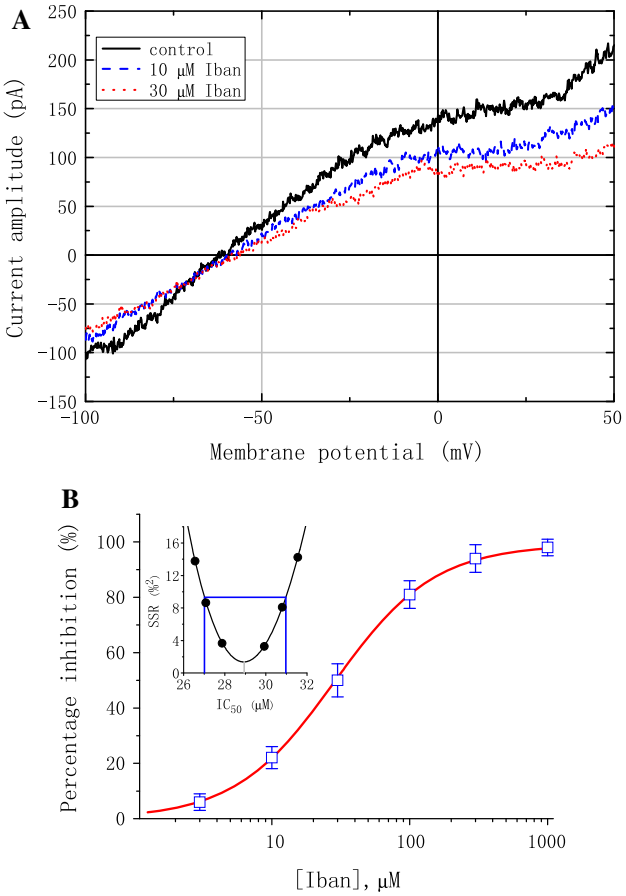

Fig. 2 Effect of Iban on voltage-gated K^+ current (I_K) in RAW 264.7 cells. In these experiments, a holding potential was set at −50 mV and the long lasting ramp pulses from −100 to +50 mV with a duration of 1 s were applied at a rate of 0.05 Hz to the cell examined. **a** Original current traces obtained with or without addition of Iban (3 and 10 μM). **b** Concentration response curve for Iban-induced inhibition of I_K (mean ± SEM; $n = 8$–12 for each point). The I_K amplitude at the level of +50 mV obtained with or without addition of difference concentrations of Iban was measured during these experiments. The smooth line represents the best fit of data to the sigmoidal Hill equation described under Materials and Methods. The values for IC_{50}, maximally inhibited percentage of I_K, and Hill coefficient were 28.9 μM, 99 %, and 1.1, respectively. The inset in (**b**) shows confidence assessment of best-fit parameter values. The parameter range corresponds to the approximate 95 % confidence intervals. Vertical gray line marks the IC_{50} value at which the sum of squared residuals (SSR) amounts to 1.392 $\%^2$

sides of the minimum, the IC_{50} value was determined with a high confidence. Thus, our results strongly indicate that Iban can exert a depressant action on the amplitude of I_K in these cells.

Comparison Among the Effects of Iban, TRAM-34, DCEBIO, and Iban plus Ionomycin on I_K

We next sought to determine the effects of Iban and other related compounds on the amplitude of I_K in RAW 264.7 cells. As depicted in Fig. 3, when cells were exposed to

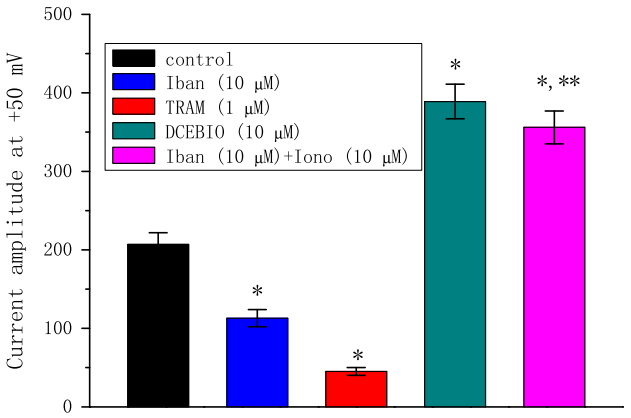

Fig. 3 Summary of the data showing effects of Iban, TRAM-34, DCEBIO, and Iban plus ionomycin on I_K in RAW 264.7 cells (mean ± SEM; $n = 7$–9 for each bar). Current amplitude was measured at the level of +50 mV. In the experiments on Iban plus ionomycin, ionomycin was subsequently applied in continued presence of Iban. TRAM: 1 μM TRAM-34. Iono: 10 μM ionomycin. *Significantly different from control ($P < 0.05$). **Significantly different from Iban (10 μM) alone group ($P < 0.05$)

TRAM-34 (1 μM), I_K amplitude at +50 mV was diminished by approximately 85 %. Addition of DCEBIO (10 μM) was found to increase current amplitude measured at the same level of voltage significantly. TRAM-34 was reported to be a potent inhibitor of IK_{Ca} channels, while DCEBIO can increase the activity of IK_{Ca} channels (Wulff et al. 2000, 2007). Moreover, in continued presence of Iban (10 μM), subsequent application of ionomycin (10 μM), a Ca^{2+} ionophore (Wu et al. 2011), was able to effectively reverse Iban-mediated inhibition of I_K in these cells. Neither iberiotoxin (200 nM) nor apamin (200 nM) produced inhibitory effects on I_K in RAW 264.7 cells. The results led us to suggest that Iban can interact largely with IK_{Ca} channels to suppress the amplitude of I_K.

Inhibitory Effect of I_K Caused by Loading the Cell via the Patch Pipette with Iban

In attempts to determine whether the effect on I_K inhibited by Iban acts through intracellular surface, additional experiments were conducted in the cells that were loaded with Iban by including the compound (10 μM) in the filling solution of the recording pipette. Time course in the change of current amplitude measured at the end of each depolarizing pulse was derived and plotted. Intracellular dialysis with Iban (10 μM) significantly decreased I_K amplitude at the level of +30 mV from 109 ± 13 to 19 ± 5 pA ($n = 9$, $P < 0.05$). Moreover, during intracellular dialysis of Iban (10 μM), subsequent addition of ionomycin (10 μM) to the cell reversed Iban-mediated inhibition of I_K, as evidenced by significant increase of current amplitude to 73 ± 16 pA ($n = 7$, $P < 0.05$).

Effect of Iban on I_K in RAW 264.7 Cells Preincubated with 17β-Estradiol

Estrogen has been recognized to exert an anti-resorptive activity in bone mass and to be effective in the management of osteoporosis (Gallagher and Tella, 2013; Mosekilde et al. 2013). One would expect that the osteoclasts exposed to 17β-estradiol could alter the effect of Iban on their functional activity. For this reason, effect of Iban on I_K was further evaluated in 17β-estradiol-treated cells. As shown in Fig. 5, in RAW 264.7 cells preincubated with 17β-estradiol for 12 h, the inhibitory effect of Iban on *I–V* relationship of I_K became little altered. For example, in cells pretreated with 17β-estradiol (1 μM), Iban at a concentration of 30 μM was capable of reducing I_K amplitude at the level of +30 mV to 86 ± 14 pA from a control of 195 ± 25 pA ($n = 8$, $P < 0.05$). There was no significant difference in the magnitude of Iban-inhibited I_K between control cells and cells treated with 17β-estradiol. Therefore, in 17β-estradiol-treated RAW 264.7 cells, addition of Iban can still effectively suppress the amplitude of I_K.

Iban Suppressed IK_{Ca}-Channel Activity Measured from RAW 264.7 Cells

In order to evaluate how Iban can interact with ion channels to depress I_{K-} amplitude, single-channel current recordings were further performed. In these experiments, cell-attached configuration was made and cells were bathed in normal Tyrode's solution containing 1.8 mM $CaCl_2$. As shown in Fig. 6, under our experimental conditions, the activity of IK_{Ca} channels can be readily detected, as described previously in different types of cells (Komarova et al. 2001; Morales et al. 2013; Shen et al. 2007; Wu et al. 1998). As Iban at a concentrations of 30 or 100 μM was applied to the bath, channel activity was progressively decreased (Fig. 6). For example, the presence of Iban (30 μM) significantly reduced the probability of IK_{Ca}-channel openings by 52 ± 4 % from 0.034 ± 0.03 to 0.17 ± 0.02 ($n = 9$, $P < 0.05$). Similar to the effect of Iban, TRAM-34 (3 μM) applied to the bath was effective at suppressing channel activity significantly. Moreover, in continued presence of 100 μM Iban, further addition of ionomycin (10 μM) reversed Iban-mediated inhibition of IK_{Ca} channels as evidenced by a significant increase in channel activity to 0.20 ± 0.02 ($n = 8$, $P < 0.05$).

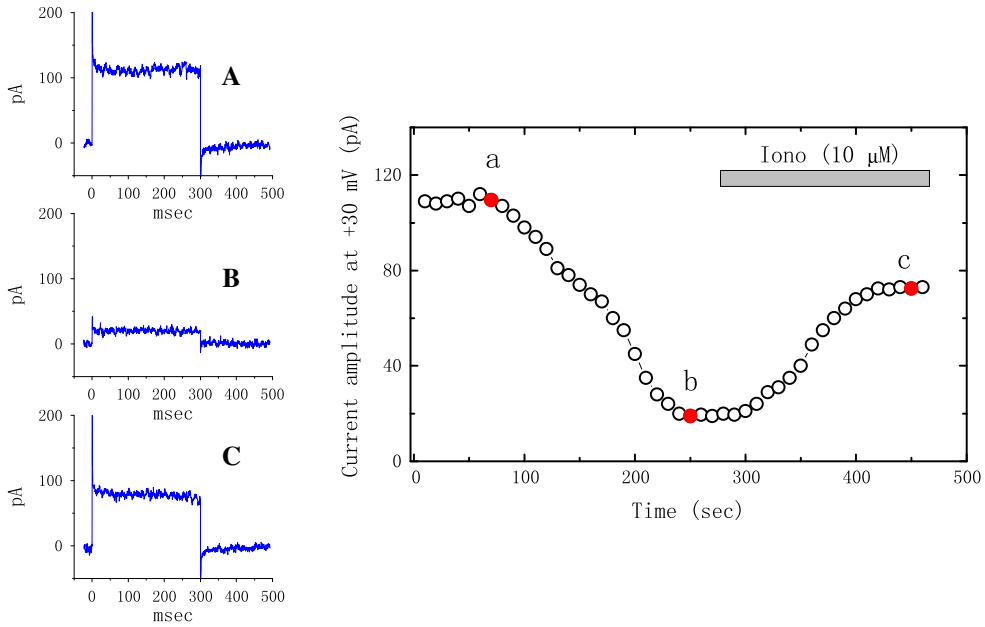

Fig. 4 Inhibitory effect on I_K caused by loading a RAW 264.7 cell with Iban (10 μM) in the recording pipette and by extracellular addition of ionomycin. The cell examined was held at −50 mV and depolarizing step to +30 mV with a duration of 300 ms at a rate of 0.1 Hz was repetitively delivered. Immediately after the membrane rupture emerges, current amplitudes under whole-cell configuration were recorded. Time course in the change of current amplitudes measured at the end of each depolarizing pulse is illustrated. Original current traces in the *left side* which are marked by labels (**a**, **b**, and **c**) correspond to the time course shown in the *right side*. Horizontal bar shown above denotes the addition of 10 μM ionomycin (Iono)

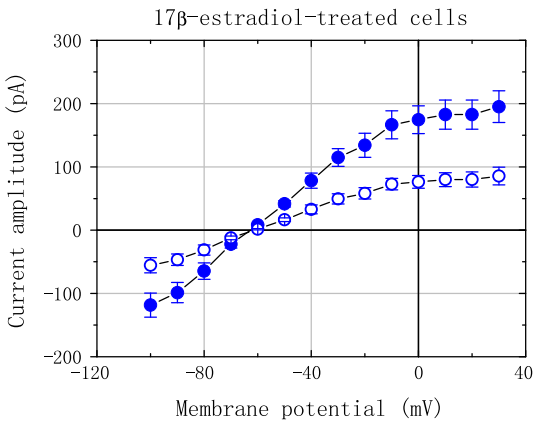

Fig. 5 Inhibitory effect of Iban on averaged *I–V* relations of I_K in 17β-estradiol-treated RAW 264.7 cells. In these experiments, RAW 264.7 cells were preincubated with 17β-estradiol (1 μM) for 12 h. In each cell examined, I_K was elicited from −50 mV to different voltages ranging from −100 to +30 mV with 10-mV increments. Each point represents the mean ± SEM (n = 6–9). *Filled circle* control; *open circle* in the presence of Iban (30 μM). Note that cell exposure to Iban remains effective at suppressing the amplitude of I_K in 17β-estradiol-treated cells

Effect of Iban on IK_{Ca}-Channel Activity Measured at Different Levels of Membrane Potential

The effect of Iban on the activity of IK_{Ca} channels at different membrane potentials was also evaluated. The plots of single-channel amplitude as a function of holding potential were derived and constructed. Figure 7a illustrates the *I–V* relationships of IK_{Ca} channels elicited by the ramp pulse with or without addition of 30 μM Iban. The single-channel conductance calculated from a linear *I–V* relationship between the absence and presence of Iban was not noted to differ significantly (34.2 ± 0.5 pS [in the absence of Iban], n = 9 versus 34.1 ± 0.6 pS [in the presence of Iban], n = 9, $P > 0.05$). The results thus showed that, in parallel with recent observations (Jones and Birchard, 2014), the IK_{Ca} channels were functionally expressed in RAW 264.7 cells and that they were sensitive to block by Iban or TRAM-34.

The voltage-dependent relation was further determined using the Woodhull equation described in Materials and Methods (Clark et al. 1995; Dunn, 1998). The values of K_0 and δ required for the inhibitory effect of Iban on IK_{Ca} channels in these cells were calculated to be 28.6 μM and 0.18, respectively (Fig. 7b). Such K_0 value is lower than IC_{50} value (i.e., 29.8 μM). These results prompted us to indicate that the inhibitory effect of this drug on the open probability of IK_{Ca} channels observed in RAW 264.7 cells is dependent on the Iban concentration as well as on changes in membrane potential.

Effect of KN-93 and KN-93 Plus Iban on IK_{Ca} Channels

The activity of calmodulin (CaM) known to form $K_{Ca}3.1$-CaM complex due to an electrostatic interaction was

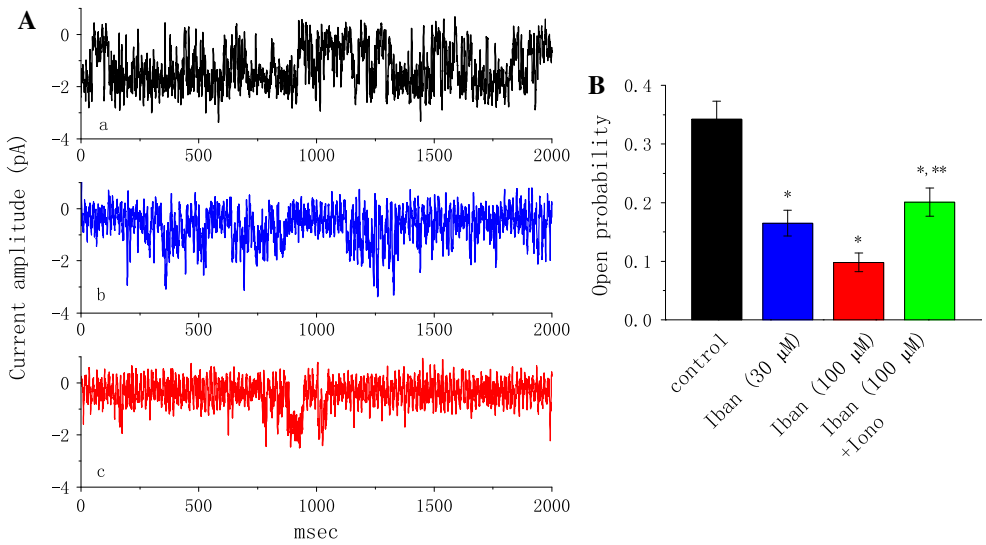

Fig. 6 Effect of Iban on the activity of IK_{Ca} channels in RAW 264.7 cells. In these experiments, cells were bathed in normal Tyrode's solution contained 1.8 mM $CaCl_2$. Cell-attached current recordings were made and each cell was constantly held at 0 mV relative to the bath. **a** Original IK_{Ca}-channel currents obtained with or without addition of Iban. Downward deflection indicates the opening event of the channel. **a** control; **b** 30 μM Iban; **c** 100 μM Iban. **b** Summary of the data showing effects of Iban (30 and 100 μM) and Iban (100 μM) plus ionomycin (Iono; 10 μM) on the probability of IK_{Ca}-channel openings (mean ± SEM; $n = 8$–10 for each bar). *Significantly different from control. **Significantly different from Iban (100 μM) alone group

previously demonstrated to influence Ca^{2+} sensitivity and gating kinetics of IK_{Ca}-channel openings (Jensen et al. 2001; Morales et al. 2013). We further examined whether the inhibitory effects of KN-93 and Iban on these channels can operate to be additive. KN-93 was reported to suppress the activity of CaM-dependent protein kinase (Anderson et al. 1998). Interestingly, as shown in Fig. 8, KN-93 (30 μM) alone decreased the channel open probability significantly; however, a subsequent addition of Iban (30 μM) was not found to diminish channel activity further. KN-93 (30 μM) significantly decreased the probability of channel openings from 0.35 ± 0.04 to 0.15 ± 0.01 ($n = 8$, $P < 0.05$). However, there was no significant difference in channel activity between the presence of KN-93 alone and KN-93 plus Iban [0.15 ± 0.01 ($n = 7$) vs. 0.15 ± 0.012 ($n = 7$), $P > 0.05$]. The experimental results thus indicate that the inhibition by KN-93 and Iban of single IK_{Ca} channel is not additive in RAW 264.7 cells.

Lack of Iban to Influence Inwardly Rectifying K^+ Current ($I_{K(IR)}$) in RAW 264.7 Cells

Earlier reports have clearly shown the presence of $I_{K(IR)}$ in RAW 264.7 cells (Tsai et al. 2013; Wang et al. 2012). We also investigated whether Iban can exert any effects on $I_{K(IR)}$ functionally expressed in these cells. These experiments were conducted in the cells bathed in Ca^{2+}-free Tyrode's solution. Each cell was held at −50 mV and different voltage pulses ranging from -120 to +30 mV in 10-mV increments were applied. We failed to show that Iban at a concentration of 30 μM exerts any effect on the *I–V* relationship of $I_{K(IR)}$ in these cells (Fig. 9). However, in continued presence of 30 μM Iban, subsequent application of $BaCl_2$ (1 mM) was effective at suppressing the amplitude of $I_{K(IR)}$ measured throughout the entire voltage-clamp step. Therefore, unlike Ca^{2+}-activated K^+ current, the $I_{K(IR)}$ is not vulnerable to block by Iban.

Effect of Iban on Resting Potential in RAW 264.7 Cells

Any changes in membrane potential can play a role in regulating the sensitivity of osteoclast Ca^{2+} influx and the level of intracellular Ca^{2+}. In another set of experiments, the effect of Iban on membrane potential was investigated in this study. Cells were bathed in normal Tyrode's solution and the recording pipette was filled with K^+-containing solution. Under current-clamp recordings, RAW 264.7 cells had a resting membrane potential of -63 ± 5 mV ($n = 23$). The typical effect of Iban on membrane potential in these cells is illustrated in Fig. 10. Addition of Iban (10 μM) depolarized the cells, as evidenced by a significant change in resting potential from −64 ± 4 to −54 ± 4 mV ($n = 9$, $P < 0.05$). After washout of this drug, the resting potential returned to −58 ± 4 mV ($n = 6$). In continued presence of Iban (10 μM), further application of DCEBIO (10 μM) was able to counteract Iban-mediated membrane depolarization to −59 ± 3 mV ($n = 7$, $P < 0.05$). Therefore, it is likely from these experiments that Iban-mediated

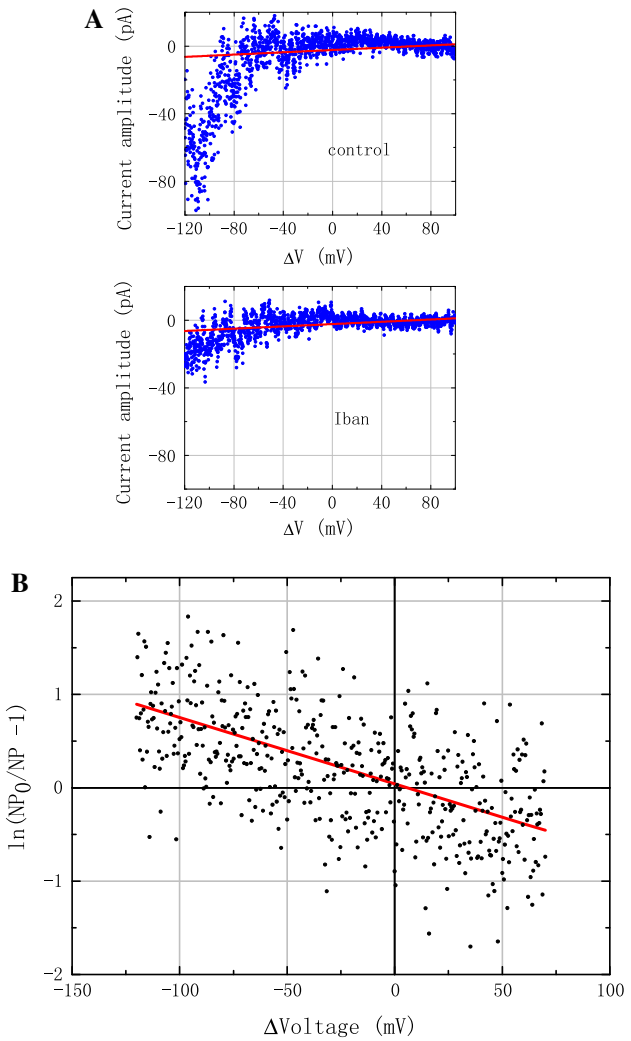

Fig. 7 Voltage dependence of Iban-mediated inhibition of IK_{Ca} channels in RAW 264.7 cells. **a** The relationship of current amplitude versus potential (i.e., Δ voltage) in the absence and presence of Iban (30 μM). In these experiments, RAW 264.7 cells were bathed in normal Tyrode's solution containing 1.8 mM $CaCl_2$. The cell examined was held at −50 mV relative to the bath and the voltage ramp pulses from −120 to +40 mV with a duration of 1 s were applied. As the patch potential is the sum of the resting potential plus the pipette potential, these currents reverse at approximately +69 mV. The straight lines with a reversal potential of +69 mV indicate the *I–V* relationships of single IK_{Ca} channels in the absence (*upper*) and presence (*lower*) of 30 μM Iban. Note that change in single-channel conductance was not demonstrated during exposure to Iban. **b** Voltage dependence of Iban-stimulated IK_{Ca} channels in RAW 264.7 cells. The activation curves were obtained when the ramp pulses were applied from −120 to +100 mV with a duration of 2 s at a rate of 0.02 Hz. The probability of IK_{Ca}-channel openings measured at different levels of membrane potential was obtained during exposure to 30 μM Iban. The data were fitted by the Woodhull equation described under Materials and Methods. The values of K_0 (i.e., the equilibrium constant at 0 mV) and δ (i.e., the fraction of membrane potential sensed by Iban at its binding site within the channel) required for the inhibitory effect of Iban on IK_{Ca} channels were calculated to be 28.6 and 0.18 μM, respectively

membrane depolarization in RAW 264.7 cells results primarily from its interactions with IK_{Ca} channels to depress the amplitude of I_K.

Effect of Iban on LPS-Induced Migration Ability in RAW 264.7 Cells

With the aid of Boyden chamber cell migration assay, treatment of cells with LPS (0.5 μg/ml) for 6 h was noted to increase the migration ability significantly. However, after cells were treated with the different concentrations of Iban for 6 h, the migration ability was drastically impaired. Incubation with LPS plus Iban for 6 h significantly decreased macrophage migration ability as compared with LPS alone (Fig. 11). For example, migration ability induced by LPS alone was significantly reduced 51 ± 12 % and 28 ± 9 % in the presence of 30 and 100 μM Iban, respectively. The results showed that Iban could depress LPS-induced migration ability in a concentration-dependent manner.

Discussion

The major findings of this study are as follows. First, Iban, a bisphosphonate, was effective at decreasing the amplitude of whole-cell I_K in a concentration-dependent manner in RAW 264.7 osteoclast progenitor cells. Second, Iban-mediated inhibition of I_K was reversed by ionomycin and an intracellular dialysis with Iban progressively suppressed the I_K amplitude. Third, in 17β-estradiol-treated cells, Iban-mediated inhibition of I_K remained effective. Fourth, Iban was able to suppress the activity of IK_{Ca} channels in a voltage-dependent manner despite its inability to alter single-channel conductance. Fifth, Iban per se was unable to perturb the amplitude of $I_{K(IR)}$ throughout the entire voltage-clamp steps examined. Sixth, this drug can depolarize the cell and inhibit LPS-induced migration. Collectively, findings from our study suggest the essential role of IK_{Ca} channels on Iban-induced inhibition of migratory ability of osteoclasts occurring in vivo.

The IC_{50} value for Iban-induced inhibition of I_K observed in RAW 264.7 cells was 28.9 μM. The estimated peak of plasma Iban concentration was reported to reach 5×10^3 ng/ml (around 14 μM) (Marathe et al. 2011). Because bisphosphonates like Iban were also noted to reveal a very high affinity and be able to bind to hydroxyapatite, the actual concentrations encountered by osteoclasts in vivo are likely to be much higher than that present in plasma. Iban was also capable of suppressing the activity of IK_{Ca} channels in a voltage-dependent manner.

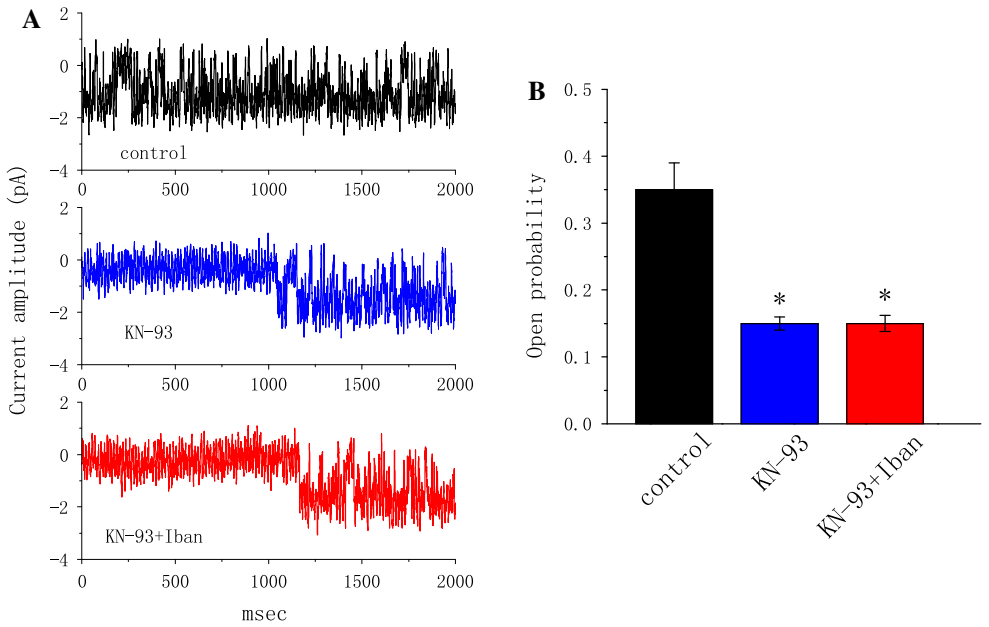

Fig. 8 Inhibitory effects of KN-93 and KN-93 plus Iban on the activity of IK_{Ca} channels recorded from RAW 264.7 cells. The experiments were conducted in normal Tyrode's solution containing 1.8 mM $CaCl_2$, and the channels were recorded from cell-attached patches of RAW 264.7 cells. **a** Original current traces recorded in control (*upper*), or in the presence of 30 μM KN-93 (*middle*) or 30 μM KN-93 plus Iban (30 μM). **b** Bar graph showing the effect of KN-93 and KN-93 plus Iban on the channel open probability (mean ± SEM; $n = 7$–12 for each bar). KN-93: 30 μM KN-93; Iban: 30 μM Iban. In the experiments with KN-93 plus Iban, Iban was subsequently applied after addition of KN-93. *Significantly different from control

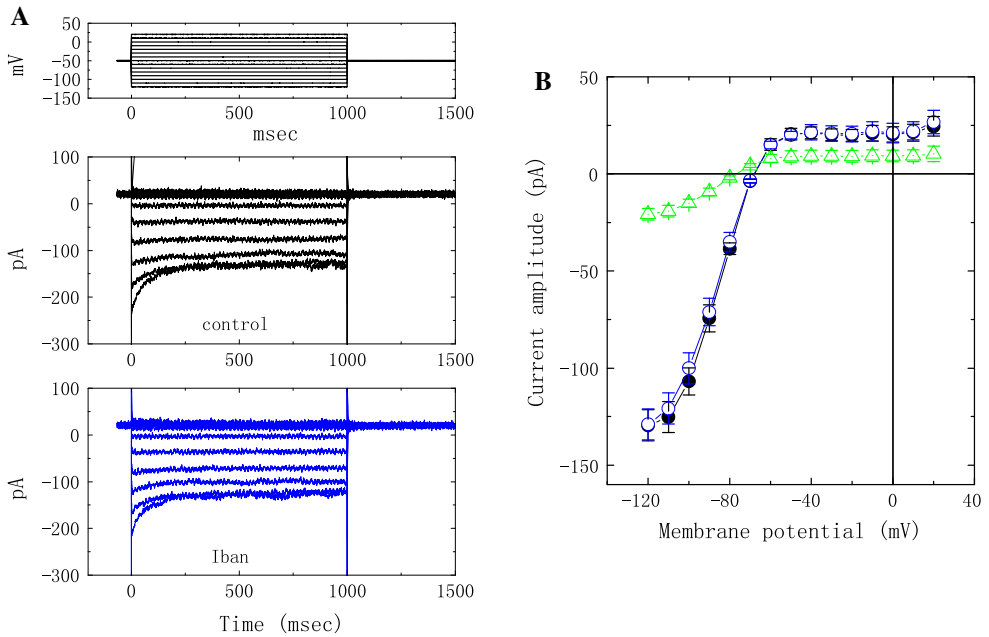

Fig. 9 Inability of Iban to alter the amplitude of inwardly rectifying K^+ current ($I_{K(IR)}$) recorded from RAW 264.7 cells. In these experiments, cells were bathed in Ca^{2+}-free Tyrode's solution. The cell examined was held at −50 mV and different voltage pulses ranging from −120 to +20 mV in 10-mV increments with a duration of 1 s were applied. **a** Original current traces obtained in the absence (*upper*) and presence (*lower*) of 30 μM Iban. The uppermost part indicates the voltage protocol used. **b** Averaged *I–V* relationships of $I_{K(IR)}$ obtained in the control (*filled circle*) and during cell exposure to 10 μM Iban (*open circle*) or 10 μM Iban plus 1 mM $BaCl_2$ (*open triangle*). Each point represents the mean ± SEM ($n = 6$–12)

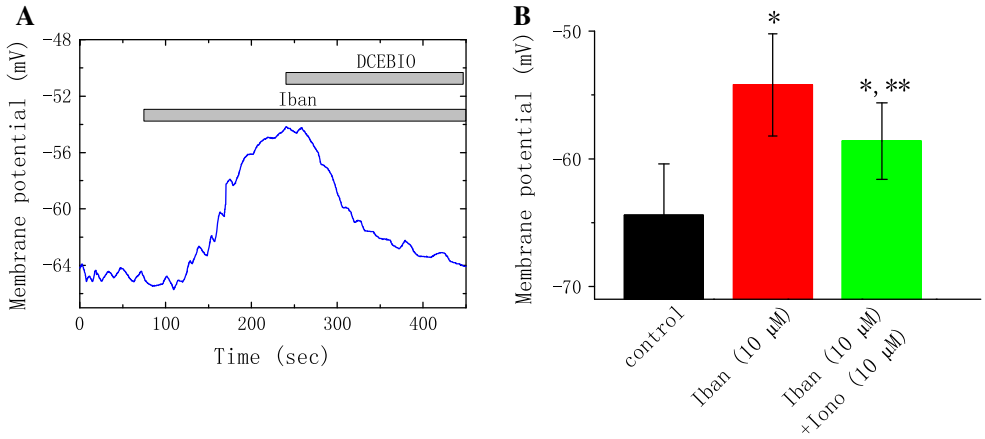

Fig. 10 Effect of Iban on the resting potential in RAW 264.7 cells. Changes in the resting potential were measured under current-clamp configuration, the experimental protocol of which was described under "Materials and Methods" section. **a** Potential trace showing the effects of Iban (10 μM) and Iban (10 μM) plus DCEBIO (10 μM) on membrane potential of a RAW 264.7 cell. Horizontal bars shown above indicate the addition of Iban or DCEBIO. **b** *Bar graph* showing summary of the effect of Iban and Iban plus DCEBIO on membrane potential in RAW 264.7 cells (mean ± SEM; $n = 7$–12 for each point). *Significantly different from control. **Significantly different from Iban alone group

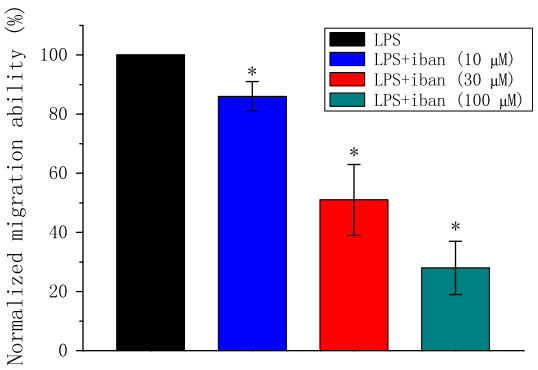

Fig. 11 Effect of Iban on LPS-induced migration ability in RAW 264.7 cells. Boyden chamber cell migration assay was used in these experiments. The cells were induced to migrate by means of the exposure to LPS (0.5 μg/ml) for 6 h. The migration ability during exposure to LPS (0.5 μg/ml) was taken to be 100 % and those in the presence of LPS plus different concentrations of Iban were measured and compared. Each bar indicates the mean ± SEM from four independent experiments with triplicate samples. *Significantly different from LPS alone group ($P < 0.05$)

The value used for inhibition of I_K is similar to those required to inhibit migration ability of these cells. Our results also provide the evidence showing that functional expression of KCNN4 ($K_{Ca}3.1$) was observed in RAW 264.7 cells (Jones and Birchard, 2014). Therefore, the effect of Iban or other structurally similar bisphosphonates on IK_{Ca} channels in osteoclasts is most likely to occur at a concentration achievable in humans. The inhibition of IK_{Ca} or KCNN4-encoded channels could be one of the important mechanisms underlying Iban-induced anti-resorptive actions.

Bisphosphonates such as alendronate were reported to activate an endogenous nonselective cation channels expressed in *Xenopus* oocytes (Shao et al. 2005). One would anticipate that Iban-induced depolarization might arise from its elicitation of such nonselective channels. However, in continued presence of Iban, subsequent addition of DCEBIO, an activator of IK_{Ca} channels, was found to reverse the ability of Iban to produce membrane depolarization. The addition of either TRAM-34 or clotrimazole also depolarized RAW 264.7 cells. Because of the activity in IK_{Ca} channels, any factors connected with increased intracellular Ca^{2+} might hyperpolarize non-excitable cells (e.g., RAW 264.7 cells), thereby producing an additional rise in the inwardly directed driving force for maintenance and facilitation of Ca^{2+} entry (Begenisich et al. 2004; Lallet-Daher et al. 2009). Indeed, we was unable to detect the presence of voltage-gated Ca^{2+} or Na^{+} channels in RAW 264.7 cells. Iban-mediated inhibition of IK_{Ca} channels in these cells can result in membrane depolarization, which consequently has the propensity to decrease the electrochemical driving force for Ca^{2+} entry. Therefore, the observed depolarization caused by Iban could be primarily a result of its inhibition of IK_{Ca} channels, rather than stimulation of nonselective channels.

An elevation in local Ca^{2+} has been previously demonstrated to trigger CaM-$K_{Ca}3.1$ interactions and to change the gating process of IK_{Ca} channels (Jensen et al. 2001; Morales et al. 2013). Our results showed that in continued presence of KN-93, an inhibitor of CaM-dependent protein kinase (Anderson et al. 1998), subsequent addition of Iban did not produce an additional reduction in the activity of IK_{Ca} channels. It is likely that Iban-mediated inhibition of

IK_{Ca} channels observed in RAW 264.7 cells is dependent on the activity of CaM-dependent protein kinase.

A previous report showed that clodronate, a bisphosphonate with no nitrogen, could raise intracellular Ca^{2+} in thyroid carcinoma cells (Yang et al. 2004). In our study, we are unable to find the ability of Iban either to increase the amplitude of whole-cell I_K or to raise the open probability of IK_{Ca} channels in RAW 264.7 cells. The stimulation of migratory ability induced by LPS was suppressed by Iban at similar concentration range. Therefore, it seems unlikely that Iban-mediated inhibition of cell migration observed in these cells results from sustained elevation of intracellular Ca^{2+}.

Inability of Iban to influence the amplitude of $I_{K(IR)}$ was seen in RAW 264.7 cells. Whole-cell I_K in RAW 264.7 was insensitive to block by chlorotoxin or margatoxin; however, it was suppressed by TRAM-34 or clotrimazole and activated by DCEBIO or ionomycin. Iban-mediated inhibition of I_K was significantly reversed by a further addition of DCEBIO. In single-channel current recordings, addition of Iban could suppress the probability of IK_{Ca}-channel openings in a voltage-dependent manner with the δ value of 0.18. Therefore, the $K_{Ca}3.1$ channels are predominant target of Iban and structurally similar agents inherently in osteoclasts (Jones and Birchard 2014; Komarova et al. 2001; Valverde et al. 2005).

In Ca^{2+}-free Tyrode's solution, our results showed that Iban-mediated inhibition of either whole-cell I_K or IK_{Ca} channels was attenuated, suggesting that its depressant action on IK_{Ca} channels is dependent on extracellular Ca^{2+}. Chemically, bisphosphonates are analogs of endogenous pyrophosphates in which the central oxygen atom is replaced by carbon, forming a P–C–P structure that is resistant to enzymatic degradation. The two phosphonate groups are recognized to be responsible for binding to bone mineral and for cell-mediated anti-resorptive activity (Ebetino et al. 2011). With the aid of ChemBio3D analysis, the minimal energies for Iban/Na complex and Iban/Ca complex were evaluated in our study. Interestingly, as Ca^{2+} ions are exposed to Iban, the total energy was greatly enhanced to -7×10^8 kcal/mol, suggesting that the degree of freedom in such molecule becomes strongly restricted; however, the value for Iban/Na complex was −111.1 kcal/mol. Consistent with previous observations (Suzuki et al. 2008), most parameters including stretch and bend energy, and energies for non-1,4-Van der Waals force and charge/dipole interaction were considerably changed, although the energy for 1,4-Van der Waals force did not differ between Iban/Na and Iban/Ca complexes (see Supplementary Table 1). Therefore, the mode of inhibitory action on IK_{Ca} channels, cell proliferation or cell migration is largely attributed to the lateral chains of the central carbon in the molecules of Iban or other structurally similar drugs (Ebetino et al. 2011; Journè et al. 2008; Komarova et al. 2001; Liu et al. 1998).

It is anticipated that the decreased activity of IK_{Ca} channels together with subsequent depolarization of the cells is responsible for the inhibitory effect of Iban on the migration of RAW 264.7 cells. However, besides the inhibition of farnesyl pyrophosphate synthase caused by Iban (Fisher et al. 2013; Pazianas, 2010; Prokopenko et al. 2014), whether its block of IK_{Ca} channels has a causal link to the inhibition of cell migration in different types of cells still remains to be further clarified. To what extent the suppression by Iban or other structurally similar bisphosphonates of IK_{Ca} channels contributes to the curtailing of bone resorption or remodeling as well as to the impact upon osteonecrotic processes remains to be further delineated.

Acknowledgments Part of the research leading to the present results was aided by a grant from the National Science Council (NSC-101-2320-B-006-009), Taiwan, through a contract awarded to S.N.W. and from the Aim for the Top University Project, National Cheng Kung University, Tainan City, Taiwan. The authors are grateful to Ming-Chun Hsu for her technical assistance in this work.

Conflict of interest No conflicts of interest, financial or otherwise, are declared by the author(s).

References

Anderson ME, Braun AP, Wu Y, Lu T, Wu Y, Schulman H, Sung RJ (1998) KN-93, an inhibitor of multifunctional Ca^{++}/calmodulin-dependent protein kinase, decreases early afterdepolarization in rabbit heart. J Pharmacol Exp Ther 287:996–1006

Begenisich T, Nakamoto T, Ovitt CE, Nehrke K, Brugnara C, Alper SL, Melvin JE (2004) Physiological roles of the intermediate conductance, Ca^{2+}-activated potassium channel Kcnn4. J Biol Chem 279:47681–47687

Clark RB, Sanchez-Chapula J, Salinas-Stefanon E, Duff HJ, Giles WR (1995) Quinidine-induced open channel block of K^+ current in rat ventricle. Br J Pharmacol 115:335–343

Diaz P, Wood AM, Sibley CP, Greenwood SL (2014) Intermediate conductance Ca^{2+}-activated K^+ channels modulate human placental trophoblast syncytialization. PLoS ONE 9:e90961

Dunn PM (1998) The action of blocking agents applied to the inner face of Ca^{2+}-activated K^+ channels from human erythrocytes. J Membr Biol 165:133–143

Ebetino FH, Hogan AL, Sun S, Tsoumpra MK, Duan X, Triffitt JT, Kwaasi AA, Dunford JE, Barnett BL, Oppermann U, Lundy MW, Boyde A, Kashemirov BA, McKenna CE, Russell RGG (2011) The relationship between the chemistry and biological activity of the bisphosphonates. Bone 49:20–33

Espinosa L, Paret L, Ojeda C, Tourneur Y, Delmas PD, Chenu C (2002) Osteoclast spreading kinetics are correlated with an oscillatory activation of a calcium-dependent potassium current. J Cell Sci 115:3837–3848

Fisher JE, Rosenberg E, Santora AC, Reszka AA (2013) In vitro and in vivo responses to high and low doses of nitrogen-containing bisphosphonates suggest engagement of different mechanisms

for inhibition of osteoclastic bone resorption. Calcif Tissue Int 92:531–538

Gallagher JC, Tella SH (2013) Controversies in osteoporosis management: antiresorptive therapy for preventing bone loss: when to use one or two antiresorptive agents? Clin Obstet Gynecol 56:749–756

Grössinger EM, Weiss L, Zierler S, Rebhandl S, Krenn PW, Hinterseer E, Schmölzer J, Asslaber D, Hainzl S, Neureiter D, Egle A, Piñón-Hofbauer J, Hartmann TN, Greil R, Kerschbaum HH (2014) Targeting proliferation of chronic lymphocytic leukemia (CLL) cells through KCa3.1 blockade. Leukemia 28:954–958

He C, Fam X, Li Y (2013) Toward ubiquitous healthcare services with a novel efficient cloud platform. IEEE Trans Biomed Eng 60:230–234

Islam S, Hassan F, Tumurkhuu G, Dagvadorj J, Koide N, Naiki Y, Mori I, Yoshida T, Yokochi T (2007) Bacterial lipopolysaccharide induces osteoclast formation in RAW 264.7 macrophage cells. Biochem Biophys Res Commun 360:346–351

Jensen BS, Strøbæk D, Olesen SP, Christophersen P (2001) The Ca^{2+}-activated K^+ channel of intermediate conductance: a molecular target for novel treatments? Curr Drug Targets 2:401–422

Jones H, Birchard Z (2014) Inhibition of KCa3.1 decreases differentiated osteoclast function in RAW264 cells. FASEB J 28:893–921

Journè F, Kheddoumi N, Chaboteaux C, Duvillier H, Laurent G, Body J-J (2008) Extracellular calcium increases bisphosphonate-induced growth inhibition of breast cancer cells. Breast Cancer Res 10:R4

Kaushal V, Koeberle PD, Wang Y, Schlichter LC (2007) The Ca^{2+}-activated K^+ channel *KCNN4*/KCa3.1 contributes to microglia activation and nitric oxide-dependent degeneration. J Neurosci 27:234–244

Kemmer G, Keller S (2010) Nonlinear least-squares data fitting in Excel spreadsheets. Nat Protocol 5:267–281

Komarova SV, Dixon S, Sims SM (2001) Osteoclast ion channels potential targets for antiresorptive drugs. Curr Pharm Des 7:637–654

Lallet-Daher H, Roudbaraki M, Bavencoffe A, Mariot P, Gackiere F, Bidaux G, Urbain R, Gosset P, Delcourt P, Fleurisse L, Slomianny C, Dewailly E, Mauroy B, Bonnal JL, Skryma R, Prevarskaya N (2009) Intermediate-conductance Ca^{2+}-activated K^+ channels (IK_{Ca1}) regulate human prostate cancer cell proliferation through a close control of calcium entry. Oncogene 28:1792–1806

Liu SI, Chi CW, Lui WY, Mok KT, Wu CW, Wu SN (1998) Correlation of hepatocyte growth factor-induced proliferation and calcium-activated potassium current in human gastric cancer cell. Biochim Biophys Acta 1368:256–266

Marathe DD, Marathe A, Mager DE (2011) Integrated model for denosumab and ibandronate pharmacodynamics in postmenopausal women. Biopharm Drug Dispos 32:471–481

McFerrin MB, Turner KL, Cuddapah VA, Sontheimer H (2012) Differential role of IK and BK potassium channels as mediators of intrinsic and extrinsic apoptotic cell death. Am J Physiol Cell Physiol 303:C1070–C1078

Morales P, Garneau L, Klein H, Lavoie MF, Parent L, Sauvé R (2013) Contribution of the KCa3.1 channel-calmodulin interactions to the regulation of the KCa3.1 gating process. J Gen Physiol 142:37–60

Mosekilde L, Vestergaard P, Rejnmark L (2013) The pathogenesis, treatment and prevention of osteoporosis in men. Drugs 73:15–29

Ohya S, Niwa S, Kojima Y, Sasaki S, Sakuragi M, Kohri K, Imaizumi Y (2011) Intermediate-conductance Ca^{2+}-activated K^+ channel, KCa3. 1, as a novel therapeutic target for benign prostatic hyperplasia. J Pharmacol Exp Ther 338:528–536

Pazianas M (2010) Osteonecrosis of the jaw and the role of macrophages. J Natl Cancer Inst 103:232–240

Prokopenko V, Kovalishyn V, Shevchuk M, Kopernyk I, Metelytsia L, Romanenko V, Mogilevich S, Kukhar V (2014) Design and synthesis of new potent inhibitors of farnesyl pyrophosphate synthase. Curr Drug Discov Technol 11:133–144

Shao W, Orlando RC, Awayda MS (2005) Bisphosphonates stimulate an endogenous nonselective cation channel in *Xenopus* oocytes: potential mechanism of action. Am J Physiol Cell Physiol 289:C248–C256

Shen AY, Tsai JH, Teng HC, Huang MH, Wu SN (2007) Inhibition of intermediate-conductance Ca^{2+}-activated K^+ channel and cytoprotective properties of 4-piperidinomethyl-2-isopropyl-5-methylphenol. J Pharm Pharmacol 59:679–685

Shin WJ, Kim YK, Song JG, Kim SH, Choi SS, Song JH, Hwang GS (2011) Alterations in QT interval in patients undergoing living donor liver transplantation. Transplant Proc 43:170–173

So EC, Wu KC, Liang CH, Chen JY, Wu SN (2011) Evidence for activation of BK_{Ca} channels by a known inhibitor of focal adhesion kinase, PF573228. Life Sci 89:691–701

Suzuki S, Hayakawa T, Kamasaki N, Okada H, Yamamoto H (2008) Conformational analysis of bisphosphonate/calcium complex. Int J Oral Med Sci 7:45–49

Toyama K, Wulff H, Chandy KG, Azam P, Raman G, Saito T, Fujiwara Y, Mattson DL, Das S, Melvin JE, Pratt PF, Hatoum OA, Gutterman DD, Harder DR, Miura H (2008) The intermediate-conductance calcium-activated potassium channel KCa3.1 contributes to atherogenesis in mice and humans. J Clin Invest 118:3025–3037

Tsai KL, Chang HF, Wu SN (2013) The inhibition of inwardly rectifying K channels by memantine in macrophages and microglial cells. Cell Physiol Biochem 31:938–951

Valverde P, Kawai T, Taubman MA (2005) Potassium channel-blockers as therapeutic agents to interfere with bone resorption of periodontal disease. J Dent Res 84:488–489

Wang CL, Tsai ML, Wu SN (2012) Evidence for mitoxantrone-induced block of inwardly rectifying K^+ channels expressed in the osteoclast precursor RAW 264.7 cells differentiated with lipopolysaccharide. Cell Physiol Biochem 30:687–701

Wu SN, Yu HS, Jan CR, Li HF, Yu CL (1998) Inhibitory effects of berberine on voltage- and calcium-activated potassium currents in human myeloma cells. Life Sci 62:2283–2294

Wu SN, Wu PY, Tsai ML (2011) Characterization of TRPM8-like channels activated by the cooling agent icilin in the macrophage cell line RAW 264.7. J Membr Biol 241:11–20

Wulff H, Miller MJ, Hänsel W, Grissmer S, Cahalan MD, Chandy KG (2000) Design of a potent and selective inhibitor of the intermediate-conductance Ca^{2+}-activated K^+ channel, *IKCa1*: a potential immunosuppressant. Proc Natl Acad Sci 97:8151–8156

Wulff H, Kolski-Andreaco A, Sankaranarayanan A, Sabatier JM, Shakkottai V (2007) Modulators of small- and intermediate-conductance calcium-activated potassium channels and their therapeutic indications. Curr Med Chem 14:1437–1457

Yang DM, Chi CW, Chang HM, Wu LH, Lee TK, Lin JD, Chen ST, Lee CH (2004) Effects of clodronate on cancer growth and Ca^{2+} signaling of human thyroid carcinoma cell lines. Anticancer Res 24(3a):1617–1623

Zhang W, Yang DL, Wang YX, Wang HW, Zhen ZJ, Zhang YZ, Shen Y (2013) In vitro osteoclast-suppressing effect of sodium ibandronate. Chin Med J 126:751–755